Faraday Discussions

Cite this: *Faraday Discuss.*, 2024, **250**, 162

ROYAL SOCIETY OF CHEMISTRY

PAPER

View Article Online
View Journal | View Issue

Singlet fission is incoherent in pristine orthorhombic single crystals of rubrene: no evidence of triplet-pair emission†

David G. Bossanyi, *[a] Maik Matthiesen,[b] Rahul Jayaprakash,[a] Sayantan Bhattacharya,[c] Jana Zaumseil[b] and Jenny Clark *[a]

Received 8th September 2023, Accepted 20th September 2023
DOI: 10.1039/d3fd00150d

Singlet fission (SF) and its inverse, triplet–triplet annihilation (TTA), are promising strategies for enhancing photovoltaic efficiencies. However, detailed descriptions of the processes of SF/TTA are not fully understood, even in the most well-studied systems. Reports of the photophysics of crystalline rubrene, for example, are often inconsistent. Here we attempt to resolve these inconsistencies using time-resolved photoluminescence and transient absorption spectroscopy of 'pristine' rubrene orthorhombic single crystals. We find the reported time-resolved photoluminescence behaviour that hinted at triplet-pair emission is found only at specific sites on the crystals and likely arises from surface defects. Using transient absorption spectroscopy of the same crystals, we also observe no evidence of instantaneous generation of triplet-pair population with ~100 fs excitation, independent of excitation wavelength (532 nm, 495 nm) or excitation angle. Our results suggest that SF occurs incoherently on a relatively slow (picosecond) timescale in rubrene single crystals, as expected from the original theoretical calculations. We conclude that the sub-100 fs formation of triplet pairs in crystalline rubrene films is likely to be due to static disorder.

1. Introduction

Photon up- and down-conversion are two promising strategies for pushing photovoltaic efficiencies beyond the Shockley–Queisser limit,[1] but achieving efficient spectral conversion remains challenging. In molecular materials, singlet fission (SF), and its reverse, triplet–triplet annihilation (TTA), offer potential solutions.[2] In SF, a high-energy singlet (spin-0) exciton (S_1) converts to a pair of low-energy triplet (spin-1) excitons ($T_1 + T_1$).[3,4] In TTA, the process is reversed.

[a]*Department of Physics and Astronomy, University of Sheffield, Hounsfield Road, Sheffield S3 7RH, UK. E-mail: jenny.clark@sheffield.ac.uk*
[b]*Institute for Physical Chemistry, Heidelberg University, Heidelberg, Germany*
[c]*Department of Life Sciences, Imperial College, London SW15 4JD, UK*

† Electronic supplementary information (ESI) available. See DOI: https://doi.org/10.1039/d3fd00150d

SF and TTA are generally accepted to proceed *via* intermediate triplet-pair states ((TT), $(T\cdots T)$)[5,6] but the details of their formation and evolution are not yet fully described,[7,8] even in archetypal SF/TTA materials such as crystalline pentacene and rubrene.[7–27]

1.1 Literature review: is singlet fission in single rubrene crystals fast (sub-picosecond) or slow?

Rubrene, whose structure is shown in Fig. 1a, is an example of a well-studied and archetypal SF/TTA material[10–27] for which the SF process is still debated.[13] In orthorhombic single crystals, for example, the peculiar symmetry of the C_{2h} π-stacking, shown in Fig. 1b, means that electronic coupling between S_1, charge-transfer (CT) and triplet-pair states should vanish. In this case, SF can only occur through coupling to symmetry-breaking vibrations and is predicted to proceed relatively slowly (incoherently) on picosecond timescales,[18,28] presumably generating weakly-exchange-coupled or mixed-spin triplet-pair states $(T\cdots T)^{1}$.[17,29] Recent spectroscopic studies on single rubrene crystals, however, are contradictory and many do not obviously support this theoretical hypothesis.[10–16,18–24,27]

For example, while some transient absorption[15,20] and transient grating pump–probe experiments[24] of rubrene crystals appear to support the calculations, showing triplet-pair population increasing approximately exponentially following photo-excitation (~2 ps time-constant), other studies instead report near-instantaneous (instrument-limited, *i.e.* <25 fs) formation of triplet-pair signatures in rubrene single crystals.[21–23,27] The latter signatures are not predicted by the calculations[18,28] and current explanations for this surprising observation differ. The details of the proposed mechanisms and the discrepancies between them are nicely described in a recent review article.[13] Broadly, it is suggested that at points on the potential energy surface, mixing between the diabatic S_1 and triplet-pair states is allowed, due to vibronic coupling, and potentially *via* charge-transfer (CT) states. Depending on the strength of the coupling, this may enable direct, 'coherent' excitation of both S_1 and triplet-pair states,[21] supported by recent calculations.[31] In this case, pure-spin exchange-coupled triplet-pair states, ^{1}(TT), should be formed and we might therefore expect to observe ^{1}(TT) emission.

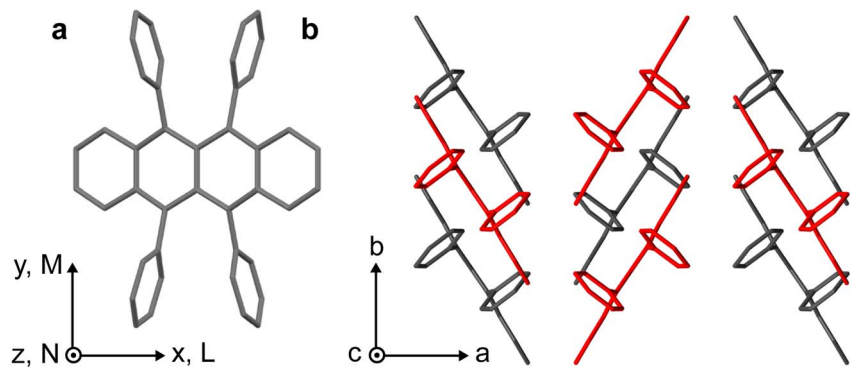

Fig. 1 Crystal structure of rubrene. (a) Molecular structure of rubrene, indicating the molecular coordinate system. (b) Orthorhombic crystal structure of rubrene obtained from ref. 30. Molecules coloured red are displaced along the *c*-axis.

1.2 Literature review: hunting for ^{1}(TT) emission: time-resolved photoluminescence of rubrene single crystals

^{1}(TT) emission has been observed in similar materials,[7,32] where it was shown to occur *via* vibronic Herzberg–Teller mixing (intensity borrowing) between the triplet-pair state and the nearby bright S_1 state.[32,33] According to the Herzberg–Teller model, the first-order TT dipole moment is given by:[34,35]

$$\mu_{S_0\text{-}TT} = \sum_{\alpha} \mu^{e}_{S_1}(Q_0) \left(\frac{\left\langle \psi_{S_1} \left| \frac{\partial H}{\partial Q_\alpha} \right| \psi_{TT} \right\rangle}{E_{S_1} - E_{TT}} \right)_{Q_0} \left\langle \chi_{S_0,\nu} | Q_\alpha | \chi_{TT,\nu'} \right\rangle. \quad (1)$$

Here Q_α are symmetry-breaking vibrational modes, $|\psi_i\rangle$ are electronic wavefunctions, $|\chi_{i,\nu}\rangle$ are vibrational wavefunctions (ν is a vibrational quantum number), H is the Hamiltonian governing Coulomb repulsion between electrons and nuclei and E_{S1}, E_{TT} are the energies of the S1 and triplet-pair, respectively. From eqn (1), we see that the brightest ^{1}(TT) emission should be observed for: (i) small S_1–^{1}(TT) energy gaps and (ii) large vibronic coupling between S_1 and ^{1}(TT) through appropriate vibrational modes that break the symmetry forbidding ^{1}(TT) from emitting at the equilibrium geometry Q_0.

In crystalline rubrene, both of these criteria appear to be met: S_1 and the triplet pairs (^{1}(TT) or (T···T)) are almost isoenergetic[32,36–38] and, as mentioned above, there is recent experimental evidence of significant vibronic coupling between S_1 and the triplet pair in rubrene single crystals.[21]

Experimental hints of possible ^{1}(TT) emission can be found in studies of the photoluminescence (PL) and absorption spectroscopy of rubrene single crystals in the literature.[10,12] Ref. 10, for example, shows that the rubrene single-crystal PL spectrum at around 565 nm and around 607 nm exhibits different dynamic behaviour, suggesting that the PL may originate from more than one electronic state.[10] In that study, only the redder part of the emission spectrum was quenched by an exciton splitter deposited at the surface of a rubrene crystal, while time-resolved PL spectroscopy measurements showed that the yellow-green part of the spectrum was short-lived, with a lifetime of approximately 15 ns compared with the delayed ($\sim$1 μs) red emission.[10] As a result of these observations, the authors of ref. 10 proposed a triplet exciton origin for the redder part of the spectrum.

Excellent work by Irkhin and co-workers offers further hints.[12] They show that the strong S_0–S_1 transition dipole moment is polarised along the *M*-axis of the rubrene molecule and hence the *c*-axis of the rubrene crystal;[12] see Fig. 1 for axes. The S_0–S_1 absorption (emission) spectrum of rubrene single crystals is therefore *c*-polarized, consisting of a vibronic progression, with the 0–0 transition at 2.32 eV (2.22 eV).[12] Interestingly, rubrene crystals also possess pronounced *ab*-polarised absorption and emission. These *ab*-polarized absorption (emission) spectra appear as vibronic progressions with the same vibrational and 0–0 energy as the *c*-polarised spectra, yet with the 0–0 transition suppressed, giving the first apparent peak at 2.49 eV (2.04 eV).[12] Suppressed 0–0 transitions such as this indicate Herzerg–Teller-type emission.

These results are suggestive. One interpretation of the spectral components might be that the S_1 state is responsible for the *c*-polarised absorption/emission and

the ~isoenergetic triplet-pair state, which borrows intensity from S_1 through Herzberg–Teller coupling, gives rise to the *ab*-polarised absorption/emission. This interpretation is consistent with the exciton quenching/time-resolved PL results from ref. 10, but it cannot explain the polarization dependence of the PL spectra.[12] We would expect the ^{1}(TT) dipole moment to retain the polarisation of the state from which it borrows intensity, in this case the *M*- and hence *c*-polarised S_1.

An alternative explanation is that the *ab*-polarised absorption/emission arises from Herzberg–Teller coupling between S_1 and a higher-lying singlet state that has its dipole moment along the *L*-axis, as originally suggested.[12] A similar mechanism has been proposed to be active in other polyacenes[39–41] and the effect would be especially pronounced in rubrene due to its unique crystal structure. However, this explanation cannot account for the different quenching and dynamical behaviour of the two components.[10]

1.3 Structure of this paper

In order to test the hypothesis that an emissive ^{1}(TT) state is the source of *ab*-polarised absorption and emission in rubrene crystals, here we begin by attempting to reproduce the results of ref. 10, in which the emission at around 565 nm was initially found to decay much faster than that at 607 nm. We find that whilst we can indeed observe this effect, it occurs only at specific sites on the crystal surface and is therefore likely a result of morphological or surface inhomogeneities. We thus find no evidence of ^{1}(TT) emission in orthorhombic single crystals.

This result is interesting in the context of the transient absorption specroscopy studies mentioned above. If ^{1}(TT) is non-emissive, the matrix element that couples S_1 with the triplet-pair state through vibrational modes in eqn (1) would be expected to be small. However, as described above, recent ultrafast experiments[21] have suggested that the vibronic coupling between S_1 and the triplet-pair state is strong enough to enable ultrafast singlet fission (which is ordinarily forbidden due to the unique symmetry of the rubrene crystal[18]). Here we investigate this apparent discrepancy by studying the transient absorption spectroscopy of the same rubrene single crystals that were used for the photoluminescence study. We find no evidence in these crystals of ultrafast (sub-100 fs) singlet fission and triplet-pair formation.

2. Results

Fig. 2 shows microscope images of the two vapour-grown rubrene crystals (see Methods section, ESI†) used in this work. Crystal 1 (Fig. 2a) is a 0.7 μm thick platelet, 120 μm wide and several mm long, with few visible imperfections. Crystal 2 (Fig. 2b) is much larger, thicker, less uniform and more damaged. Optical experiments were confined to the region indicated by the red box in Fig. 2b. This region is approximately 2 μm thick.

The absorption spectra of crystals 1 and 2 are shown in Fig. 3a and b, respectively, for incidence angles of 0° and 30°. The 0° spectra are consistent with the *ab*-polarised absorption of orthorhombic rubrene single crystals.[12] The increased absorption and appearance of a peak at 532 nm upon rotation of the crystal to 30° incidence reflect the contribution of the *c*-polarised component. This demonstrates that the *M*-axes of the rubrene molecules, and hence the *c*-axis of the crystals, is normal to the substrate plane. Crystals 1 and 2 therefore have

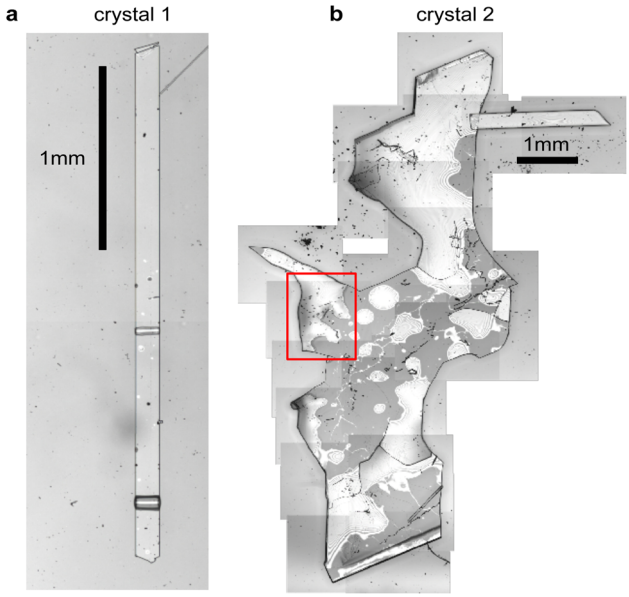

Fig. 2 Rubrene single crystals. (a and b) Microscope images of crystals 1 and 2, respectively, grown by physical vapour transport. All spectroscopic measurements of crystal 2 were conducted within the region indicated by the red box.

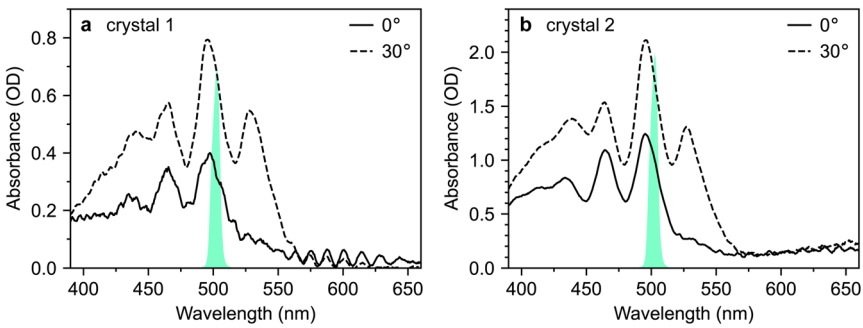

Fig. 3 Absorption spectra of rubrene single crystals. (a and b) Absorption spectra of crystals 1 and 2, respectively, at both 0° and 30° degree incidence angles. The spectra of the excitation pulses are also shown in cyan.

their largest dimensions in the *ab*-plane, as expected for vapour-grown rubrene crystals.[12] Excitation at 532 nm therefore selectively excites the *c*-polarised transition, whilst excitation at around 500 nm excites both the *c*- and *ab*-polarised transitions, with the ratio of absorptions dependent on the incidence angle.

2.1 Site-dependent anomalous photoluminescence behaviour in single crystals

Fig. 4a and b show time-gated photoluminescence spectra, normalised at 607 nm, from crystals 1 and 2 following pulsed excitation at 500 nm. The pump was

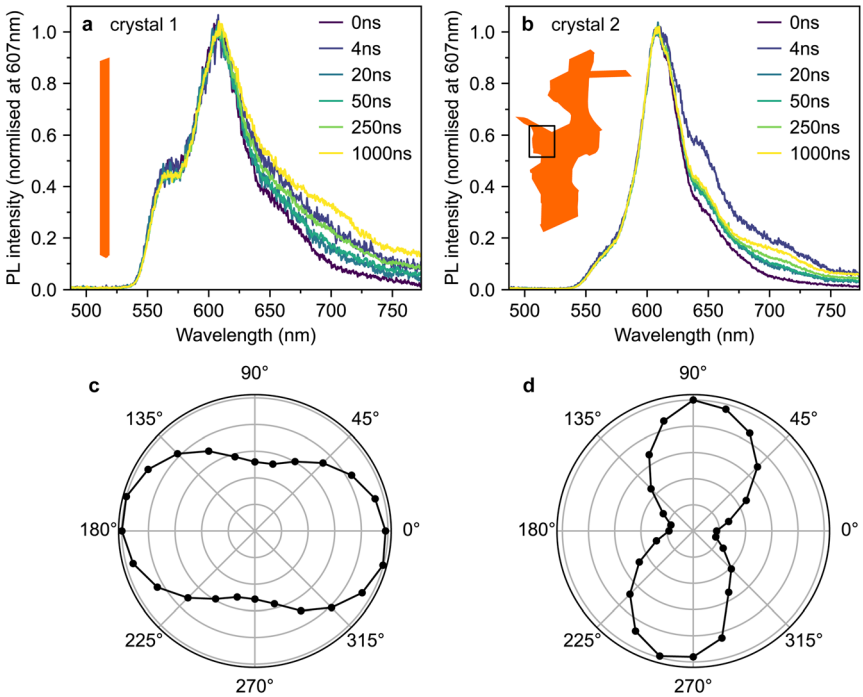

Fig. 4 Ordinary photoluminescence behaviour of rubrene crystals. (a and b) Time-gated PL spectra, normalised at 607 nm, for crystal 1 (a) and crystal 2 (b). (c and d) The dependence of the PL intensity at 607 nm on the rotation angle of a linear polariser placed before the detector. The excitation density was approximately 50 μJ cm^{-2} for all time-resolved photoluminescence (TRPL) measurements reported in this paper.

introduced at an incidence angle of 45° and therefore excites both the *c*- and *ab*-polarised absorption components. The pump spectra are shown in Fig. 3. PL (in all polarisations) was collected at normal incidence to the *ab* crystal plane (see Methods section, ESI†).

Fig. 4c and d show the dependence of the PL intensity (integrated from 0–2 μs) on the rotation angle of a linear polariser placed before the detector. In both cases, the intensity exhibits the expected $\cos^2(\theta)$ pattern associated with dipole emission. The pattern is slightly less pronounced in crystal 1 (Fig. 4c), perhaps due to some PL 'leakage' from the edges of the crystal being picked up by the collection lens.

We observe slight changes with time to the shape of the PL tail beyond 620 nm in Fig. 4a and b, which suggests small contributions from lower-lying excited states.[42] Similar low-energy bands of varying intensity are commonly observed in the PL tail of rubrene single crystals.[12,15,16,21,23,42–46] The origins of such bands are debated; suggestions include oxygen-related mid-gap states[45] or amorphous regions within the crystal.[42] We note that the PL spectra from our crystals strongly resemble the spectra from 'pristine' rubrene single crystals in ref. 12 (see Fig. S3†).

Crucially, we do not find any significant differences in temporal behaviour between 565 nm and 607 nm and therefore between the *c*- and *ab*-polarised

emission components, suggesting that at the positions measured, both components arise from the same excitonic species.

However, by scanning around the surface of crystal 2, we were able to find a spot that reproduced the behaviour observed in ref. 10, which we denote crystal 2*. The time-gated spectra from this spot (Fig. 5a) show a striking dependence on detection wavelength. A short-lived component that peaks at ~565 nm (and is hence *c*-polarised only[12]) dominates during the first few nanoseconds, before giving way to a constant spectrum resembling the *ab*-polarised emission (plus the expected *c*-polarised 'leakage' due to experimental conditions[12]). These different dynamics are clearly evident when comparing the PL decay profiles in Fig. 5b. Beyond 50 ns, the PL dynamics of crystals 2 and 2* are identical. Initially however, the band at 565 nm appears as an extra component with a lifetime of a few nanoseconds.

To investigate the origins of the two emission components evident in crystal 2*, we measured the detection polarisation anisotropy of the PL intensity, shown in Fig. 6a and b. The long-lived, mainly *ab*-polarised component of crystal 2* (red, Fig. 6a and b) shows the same expected $\cos^2(\theta)$ dipole dependence as crystals 1 and 2 (Fig. 4c and d). In contrast, the short-lived, *c*-polarised component of crystal 2* (green, Fig. 6a and b) is almost completely isotropic.

If ^{1}(TT) and S_1, respectively, are the sources of the *ab*- and *c*-polarised emission components, we would not expect significant differences in their anisotropy, nor would we expect the *c*-polarised part to be observable only at specific sites on the crystal. Instead, the measurements in Fig. 4–6 indicate that the short-lived, *c*-like component arises from a sub-population of singlet excitons found only at certain points on the crystal due to morphological inhomogeneity.

This conclusion is in agreement with results in ref. 12, where they found that micrometer-sized defects on the crystal surface within the excitation/detection region resulted in a large enhancement in the PL shoulder at 565 nm. This was attributed to the scattering of *c*-polarised PL into the detector. Such scattering would explain why we measure this emission to be isotropic. Indeed, an examination of the surface of crystal 2 (Fig. 2b) reveals that several rough, micrometer-sized microcrystals are present on the surface. An example of such a surface microcrystal is shown in Fig. 6c, and it is clear from the PL image in Fig. 6d that

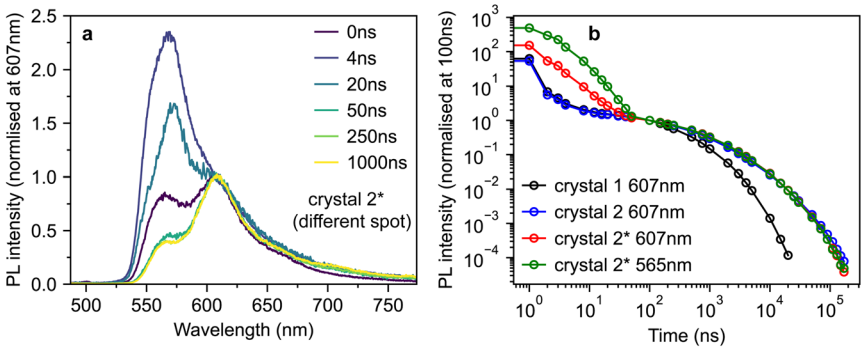

Fig. 5 Anomalous photoluminescence behaviour of rubrene crystals. (a) Time-gated PL spectra, normalised at 607 nm, for crystal 2*, a different spot on the surface of crystal 2 that exhibited similar PL behaviour to that reported in ref. 10. (b) Time-dependence of the PL intensity from crystals 1, 2 and 2* at various detection wavelengths, normalised at 100 ns.

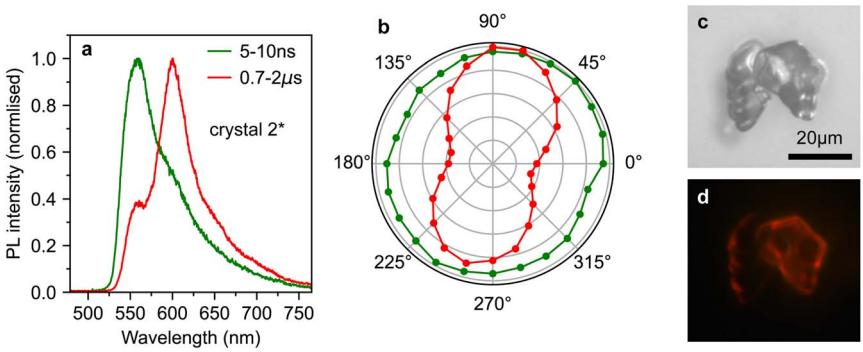

Fig. 6 Origins of anomalous photoluminescence behaviour of rubrene crystals. (a) Normalised PL spectra from crystal 2*, gated from 5–10 ns (green) and 0.7–2 μs (red). (b) The dependence of PL intensity (at 565 nm, green and 607 nm, red) on detection polariser angle for the two spectra shown in (a). (c) Microscope image of a microcrystal defect on the surface of crystal 2. Such a defect is a candidate source of the emission from crystal 2*. (d) Image of the photoluminescence from the defect shown in (c). The defect is much brighter than the bulk crystal.

these microcrystals can be significantly brighter than the bulk crystal. It therefore seems likely that such microcrystals or defects, rather than singlet and triplet origins, are the cause of the curious results in ref. 10.

We have demonstrated that there is no clear evidence of photoluminescence from the ^{1}(TT) state in rubrene single crystals, despite the small S_1–triplet-pair energy gap, suggesting that either ^{1}(TT) behaves identically to the signature attributed to S_1, which seems unlikely given the strong similarity to the S_1 spectrum in solution,[12] or the triplet pair is not emissive. Instead, our photoluminescence experiments show that previously observed differences in the behaviour of *c*-polarised and *ab*-polarised emission components are found only at particular sites on rubrene crystals. We have shown that these sites are likely to correspond to microcrystal surface defects.

This result introduces something of a conundrum. If ^{1}(TT) is non-emissive in rubrene crystals, the matrix element that couples S_1 with the triplet pair through vibrational modes in eqn (1) must be small. However, recent ultrafast experiments[21] have suggested that the vibronic coupling between S_1 and the triplet pair is strong, such that it enables ultrafast singlet fission (which is ordinarily forbidden due to the unique symmetry of the rubrene crystal[18]). We investigate this apparent discrepancy by studying the transient absorption spectroscopy of pristine rubrene crystals.

2.2 Transient absorption spectroscopy of pristine rubrene crystals demonstrates no evidence of coherent ^{1}(TT) formation

For this study, we use the same rubrene crystals shown in Fig. 2. We judged our crystals to be pristine, particularly crystal 1, by comparing their PL spectra against those reported in ref. 12, an extremely careful and comprehensive analysis of the absorption and emission properties of rubrene single crystals (see, for example, Fig. S3†). We note that the PL spectra reported by Miyata *et al.*[21] and Bera *et al.*[23] are both dominated by the 650 nm band, indicative of defective rubrene crystals.[12,42,45]

Furthermore, the PL spectrum (from platelet crystals very similar to ours) reported by Breen *et al.*[22] is dominated by a band at 565 nm. We showed above, in accordance with ref. 12, that such emission can arise from microcrystal defects on the crystal surface and is associated with changes in PL dynamics. The lack of experimental details surrounding the acquisition of the PL spectrum make interpretation difficult; however, we note that such defects can be clearly seen in the microscope image presented by Breen *et al.*[22] In fact, of the transient absorption literature reviewed above, only Ishibashi *et al.*[20] report a PL spectrum consistent with pristine rubrene crystals.[12] We will see below that potentially defective crystals may have a substantial impact on the measured transient absorption data.

Fig. 7 reproduces the absorption spectra of crystals 1 and 2 from Fig. 3. Alongside, we plot the spectra of two different pump pulses used in our transient absorption experiments. The pulse centred at 495 nm selectively excites the 0–1 transition, which includes both *ab*- and *c*-polarised components.[12] The pulse centred at 532 nm selectively excites the vibrationless 0–0 transition, which is exclusively *c*-polarised.[12]

According to the coherent mechanism proposed by Miyata *et al.*,[21] excitation using either of these pump pulses should result in instrument-limited ^{1}(TT) formation. In contrast, the incoherent pathway suggested by Breen *et al.*[22] should only be activated when the initial photo-excited state is a vibrationally dressed S_1 state. In that case, instrument-limited triplet-pair formation should be observed only when pumping at 495 nm. Comparing the dynamics of the triplet-pair population under these two excitation conditions should therefore enable us to distinguish between these two mechanisms. To obtain further confirmation of our conclusions above, that ^{1}(TT) is not responsible for the *ab*-polarised absorption component, we also performed experiments at both 0° and 30° incidence.

2.3 No instantaneous triplet-pair formation in single crystals with ~100 fs excitation

Fig. 8a and b show transient absorption spectra recorded in crystal 1 with 495 nm excitation at 0° incidence, and 532 nm excitation at 30° incidence, respectively

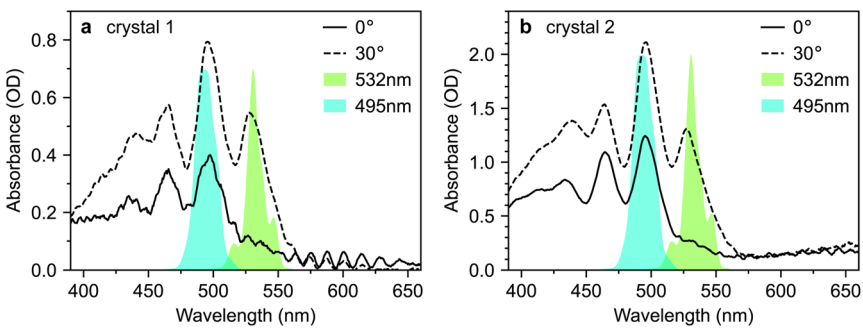

Fig. 7 Selective excitation of rubrene single crystals. (a and b) Absorption spectra of rubrene single crystals 1 and 2 at incidence angles of 0° and 30°, reproduced from Fig. 3. The 495 nm and 532 nm pump spectra used in the transient absorption experiments presented in this paper are shown. The two pump wavelengths target the 0–1 and 0–0 vibronic transitions, respectively.

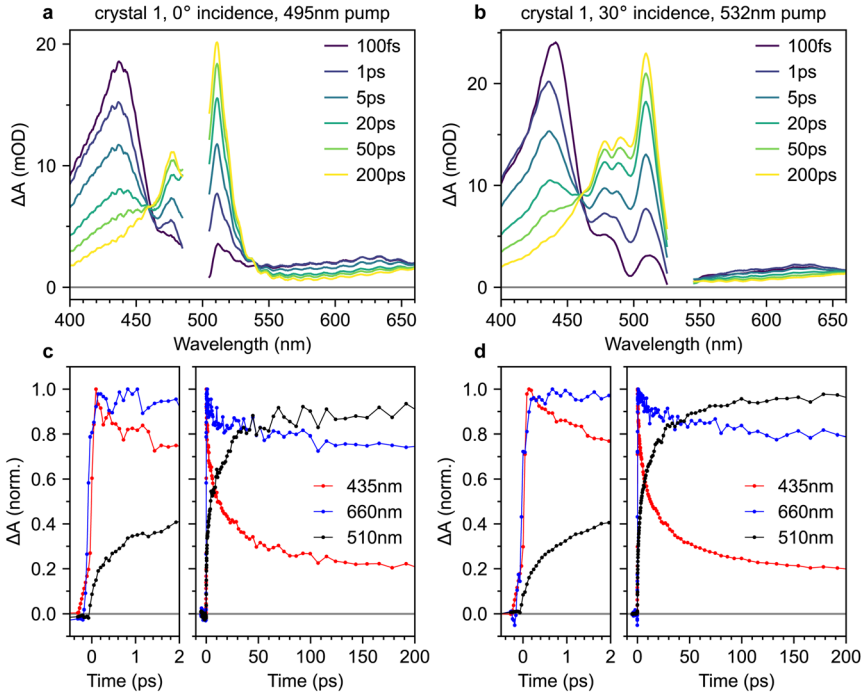

Fig. 8 Transient absorption spectroscopy of rubrene crystals. (a and b) Transient absorption spectra measured on crystal 1 at different delay times for 495 nm excitation at 0° incidence (a) and 532 nm excitation at 30° incidence (b). (c and d) Corresponding transient absorption dynamics at 435 nm (mostly S_1), 660 nm (mixture of S_1 and triplet pairs) and 510 nm (almost entirely triplet-pair population). The excitation intensity was 70 μJ cm^{-2} for all experiments reported in this paper.

(complete data sets for both crystals are shown in the ESI, Fig. S9–S12†). The band at 435 nm arises from the $S_1 \rightarrow S_3$ excited-state absorption[15,38] whilst the band at 510 nm is characteristic of $T_1 \rightarrow T_3$.[15,20–22,38] In the probe region beyond 550 nm, both singlet and triplet excited-state absorptions contribute.[21,38,47] Absorptions from charge-separated states can also be present in the spectral region around 600–900 nm.[14,48] We discount them here because they are usually observed only under ultraviolet excitation[14,15,48] and are generally short-lived,[48] unlike the persistent signal apparent at 660 nm in our measurements. We observe an isosbestic point between the singlet and triplet-pair absorption features, indicating that singlet fission is a one-to-one conversion between S_1 and a triplet pair.[15]

The transient absorption dynamics corresponding to Fig. 8a and b are plotted in Fig. 8c and d for probe wavelengths of 435 nm (mostly singlets), 660 nm (a mixture of singlets and triplet pairs) and 510 nm (almost entirely triplet pairs). The dynamics are normalised to the maximum signal at 435 nm. In Fig. S14,† we demonstrate that the dynamics at 510 nm are almost entirely uncontaminated by spectral overlap with nearby singlet bands and are thus a good measure of triplet-pair population.

We find no clear evidence of instrument-limited triplet-pair formation in Fig. 8c and d. The rise in the triplet-pair population at 510 nm starts after, and is

less steep than, the rise of the photo-excited singlet population at 435 nm. This cannot be an artefact of the chirp correction procedure (see Methods section, ESI†) because it is also later, and less steep, than the rise of the signal at 660 nm. This behaviour is the same regardless of excitation wavelength.

In order to compare our measured triplet-pair dynamics with previous measurements, we attempted to extract time constants using multi-exponential fitting. We found that whilst a bi-exponential function gave a good fit, the extracted time constants varied significantly depending on the time window used for the fit. Moving to a tri-exponential function (Fig. 11a, below) provided a much more robust set of fitting parameters. However, as a result of the large number of fitting parameters (six) and clear non-exponential behaviour, it does not make sense to talk about time constants *per se*. Nevertheless, the fitting results are instructive, particularly when we come to compare the triplet-pair dynamics to those measured for a polycrystalline film below.

A tri-exponential fit to the triplet-pair dynamics of crystal 1 (532 nm excitation, 30° incidence), shown below in Fig. 11a, yielded time constants of 0.25(3) ps (23(2)%), 1.8(4) ps (26(3)%) and 14(3) ps (51(2)%). These three values are similar to those extracted by Breen *et al.*[22] and the latter two time constants agree well with those reported by Ma *et al.*[15] and Ishibashi *et al.*[20] based on bi-exponential fitting. Our sub-picosecond component is slower than that of ref. 22 by a factor of 2–3. This might reflect differences in the instrument response time, though we reiterate that our initial triplet-pair rise is slower than the rise time of the singlet exciton signal.

For completeness, Fig. 9 compares the triplet-pair dynamics probed at 510 nm for both crystals 1 and 2 under different excitation wavelengths and incidence angles (full datasets are also shown in ESI Fig. S9–S12†). We find that the dynamics are very similar across both crystals, incidence angles and excitation wavelengths. It appears that the triplet-pair dynamics exhibit a very slightly more pronounced sub-picosecond component when the excitation wavelength is 495 nm, resulting in a marginally larger population at 2 ps. At first glance, this appears to support the conclusions of Breen *et al.*[22], that a vibrationally dressed photo-excited singlet state (only possible with 495 nm excitation in our experiment) is required to enable ultrafast triplet-pair formation. However, it is

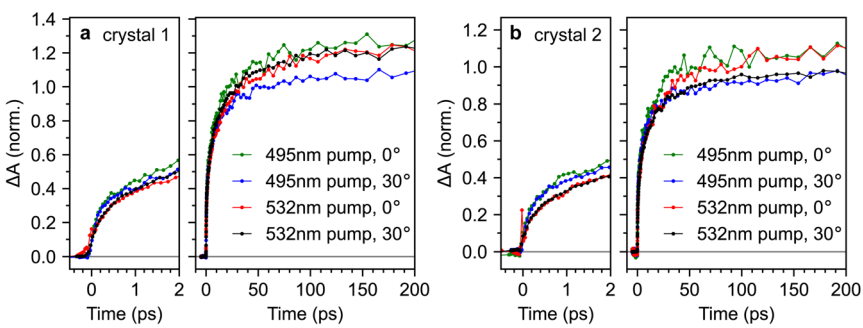

Fig. 9 Consistent triplet-pair dynamics in rubrene crystals. (a and b) Triplet-pair dynamics, probed at 510 nm for single crystals 1 and 2 respectively. No major differences were observed between different crystals, excitation wavelengths or incidence angles.

noticeable from Fig. 9 that the effect of excitation wavelength is more pronounced in crystal 2 than crystal 1. Crystal 2 is significantly more defective (see Fig. 2), suggesting that this may not be an intrinsic bulk effect.

2.4 Transient absorption spectroscopy of polycrystalline rubrene films shows instrument-limited formation of triplet pairs

Since many of the rubrene crystals reported in the literature exhibit PL spectra indicative of defects, and since we find that the effect of excitation wavelength on sub-picosecond triplet-pair formation is more pronounced in a more defective crystal, we repeated our measurements on a polycrystalline thin film. The absorption spectrum is shown in Fig. 10a and the microscope image in Fig. 10b reveals a polycrystalline texture on the micrometer length scale.

Strikingly, when comparing the transient absorption dynamics of the film and crystal in Fig. 10c, we find very clear evidence of instantaneous triplet-pair formation in the polycrystalline sample. The initial rise of the triplet-pair signal at 510 nm exactly follows the rise of the photo-excited singlet at 435 nm, likely demonstrating ^{1}(TT) formation within the instrument response. We demonstrate in Fig. S15† that this observation is not an artefact of spectral overlap. We note that the instantaneous triplet-pair formation in the polycrystalline film occurs even though the excitation wavelength is 532 nm. 532 nm is not sufficiently energetic to populate vibrationally dressed S_1 states, thereby casting doubt on the mechanism proposed by Breen *et al.*[22] to explain femtosecond singlet fission in rubrene.

We repeated the tri-exponential fitting for the triplet-pair dynamics on the polycrystalline film. The fit is shown in Fig. 11a and we extracted time constants of 0.21(5) ps (59(12)%), 1(3) ps (16(23)%) and 6(6) ps (25(27)%). The large errors on the latter two components illustrate the limitations of such fitting, but it is clear that the sub-picosecond component is significantly greater, and slightly faster, than in the bulk crystal. More instructively, in Fig. 11b, we show that for the first

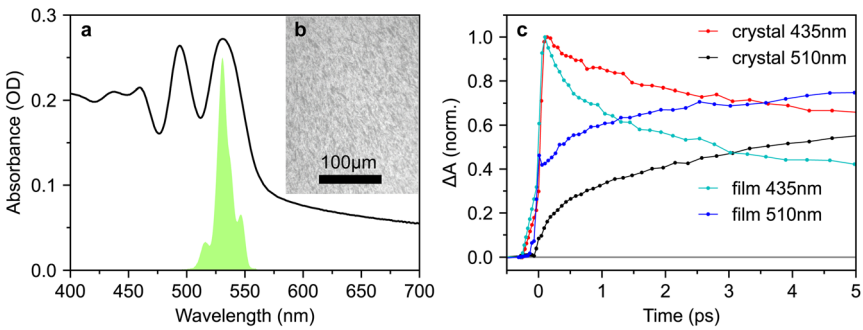

Fig. 10 Instantaneous triplet-pair formation in polycrystalline films. (a) Absorption spectrum of a polycrystalline rubrene film prepared by thermal evaporation and annealing. (b) Microscope image of the film surface, revealing a micrometer-scale polycrystalline texture. Many of the crystals appear to be oriented in the same direction. (c) Comparison of transient absorption dynamics at probe wavelengths of 435 nm and 510 nm between crystal 1 (30° incidence) and the polycrystalline film. The excitation wavelength (532 nm) and intensity (70 μJ cm^{-2}) were the same in both cases.

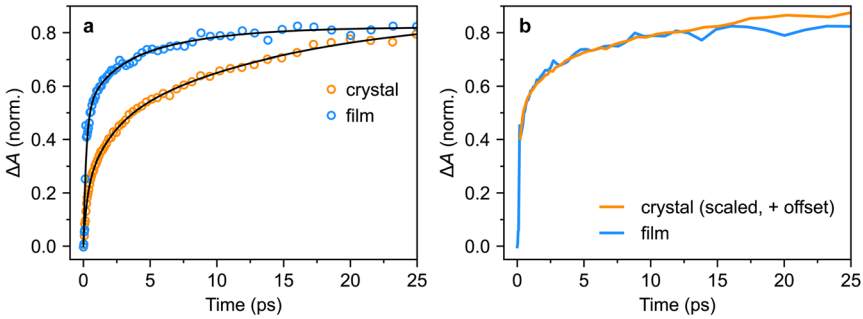

Fig. 11 Triplet-pair dynamics in crystals and films. (a) Tri-exponential fits to the triplet-pair population dynamics of crystal 1 (532 nm excitation, 30° incidence) and a polycrystalline film (also 532 nm excitation). (b) The triplet-pair dynamics of the polycrystalline film, following the instrument-limited rise to 50% of the maximum population, closely match those of the bulk single crystal when a constant offset is added to the latter.

few tens of picoseconds, the triplet-pair dynamics of the polycrystalline film can be explained as an instrument-limited initial offset of around 50% of the maximum population with subsequent dynamics that exactly match those of the bulk crystal.

For completeness, we also measured the time-resolved photoluminescence (TRPL) of our polycrystalline thin film under both 500 nm and 532 nm excitation (Fig. 12a and b respectively).

The spectra are similar in both cases and slightly blue-shifted compared with the single-crystal emission spectrum. Following 532 nm excitation (Fig. 12b), we observe a small shoulder growing in on a timescale of several nanoseconds at 630 nm. This is similar to a spectral feature previously assigned to ^{1}(TT) in rubrene thin films.[32] However, we observe no such behaviour following excitation at 500 nm (Fig. 12a). The slight changes in behaviour with excitation wavelength may be due rather to a different region of the film falling within the excitation spot across the two separate measurements. Furthermore, it is well known that defects in rubrene films can emit at around 630 nm (ref. 12). Further careful experiments are required before a concrete assignment of the polycrystalline thin-

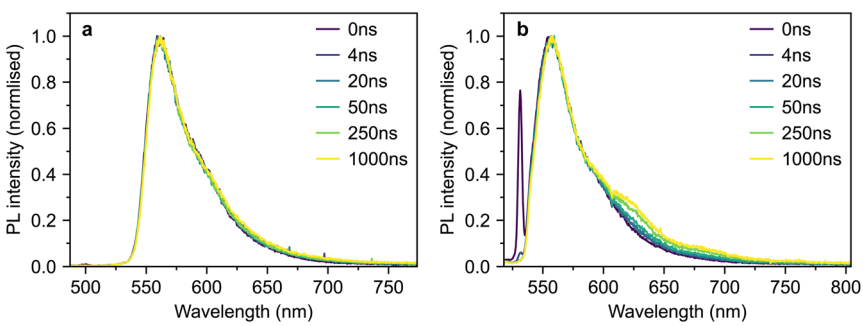

Fig. 12 TRPL of polycrystalline rubrene. (a and b) Time-gated photoluminescence spectra of a polycrystalline rubrene film following excitation at 500 nm (a) and 532 nm (b).

film photoluminescence spectrum can be made; these are beyond the scope of the current work.

3. Discussion

Our transient absorption results demonstrate that instantaneous, or instrument-limited, formation of triplet pairs following photo-excitation of crystalline rubrene occurs in polycrystalline thin films but not in bulk single crystals. Following this ultrafast rise for the film, the triplet-pair dynamics appear almost identical to those of the bulk crystal. The lack of femtosecond singlet fission in rubrene crystals is in line with expectations,[18] raising the question of what factors enable it to occur in polycrystalline films.

One possibility is that the triplet-pair state and S_1 are mixed at certain sites within the film morphology where the C_{2h} π-stacking symmetry breaks down due to static disorder, for example at grain boundaries or dislocations. At these sites, ^{1}(TT) can be formed extremely rapidly, whilst elsewhere, triplet-pair formation dynamics mimic those of the bulk crystal, as shown in Fig. 11b. It is perhaps curious then that singlet fission is reported to be completely suppressed in truly amorphous solid rubrene,[24] though this may simply be a result of weaker intermolecular couplings. Further experiments and calculations may be required to discover which intermolecular alignments are preferential for ultrafast singlet fission in rubrene.

These two proposed types of singlet fission, bulk and defect, are shown schematically in Fig. 13a and b, respectively. In the bulk (a), low-energy librational

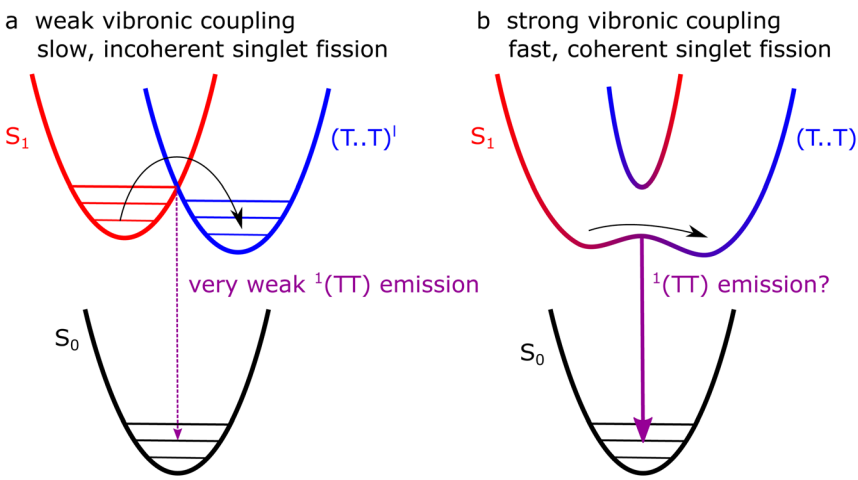

Fig. 13 Possible singlet-fission pathways in crystalline rubrene. (a) In bulk crystals, low energy modes provide weak vibronic coupling between S_1 and triplet pairs (here denoted as $(T\cdots T)^I$ as in the absence of vibronic/electronic coupling, the triplet pairs are weakly exchange-coupled and mixed-spin states). As a result, singlet fission is incoherent and slow (picosecond timescale). (b) At sites where the symmetry is broken by static disorder, S_1 and triplet pairs can become strongly mixed, allowing fast (femtosecond) coherent formation of ^{1}(TT). We might expect the strength of any Herzberg–Teller emission from ^{1}(TT) to follow the strength of vibronic coupling (purple arrows).

modes provide weak vibronic coupling between S_1 and triplet-pair states, enabling incoherent singlet fission to occur with a picosecond time constant. At sites where the symmetry constraint is broken (b), the triplet pair and S_1 may become substantially mixed. Photo-excitation at such sites results in a coherent superposition of S_1 and ^{1}(TT).

The pathways proposed in Fig. 13 suggest that photoluminescence from ^{1}(TT), enabled by vibronic coupling, or Herzberg–Teller intensity borrowing, might be present in polycrystalline thin films but, as we described above, not in single crystals. We have observed no clear ^{1}(TT) emission in the polycrystalline films (Fig. 12), but note that the emission spectra are shifted compared with both solution and crystal spectra[12] and more work is required to understand these spectra before fully ruling out ^{1}(TT) emission.

We take our results to suggest that in pristine orthorhombic single crystals, only weakly bound triplet-pair states $(T\cdots T)^l$ are formed. In samples with defect sites, on the other hand, it is likely that exchange-coupled triplet states ^{1}(TT) are formed instantaneously at the defects due to the lack of symmetry constraints. The lack of direct spectroscopic evidence of ^{1}(TT) states in defective films or crystals, however, remains to be resolved.

4. Conclusions

We have demonstrated that ultrafast instantaneous formation of triplet-pair states in crystalline rubrene occurs in polycrystalline films but not in single crystals, in contrast to recent reports. Our results are consistent with calculations showing that singlet fission in rubrene crystals is an incoherent process, occurring on the picosecond timescale, and driven by low-energy vibrational modes that weakly couple S_1 to $(T\cdots T)^l$.

We propose that the instantaneous triplet-pair formation that we readily observe in polycrystalline films arises from static disorder. At certain sites within the film morphology, molecules may be oriented in such a way as to break the symmetry and allow S_1, charge-transfer states and triplet pairs to mix. At such sites, singlet fission can be a coherent process, producing ^{1}(TT). Such mixing should result in site-dependent Herzberg–Teller emission from the ^{1}(TT) state in polycrystalline rubrene, but we could not observe it.

Our results highlight the need for more detailed experiments to investigate the dependence of singlet fission on inter-molecular geometry in rubrene and to ensure that single-crystal studies are performed on pristine samples. Our results also suggest a strategy to avoid losses in singlet-fission systems from strongly exchanged coupled ^{1}(TT) that rapidly decay radiatively and non-radiatively,[33] by designing systems in which singlet fission is symmetry-constrained, as in rubrene.

Author contributions

DGB and JC conceived of the project; DGB and MM grew the crystals with supervision from JZ; DGB grew the polycrystalline films, and performed most of the experiments and all of the analysis with supervision from JC. RJ performed the optical microscopy measurements. SB built the non-collinear parametric amplifier for these experiments. The manuscript was written by DGB and JC with input from all authors.

Conflicts of interest

There are no conflicts of interest to declare.

Acknowledgements

DGB thanks the EPSRC Centre for Doctoral Training in New and Sustainable Photovoltaics (EP/L01551X/1) for studentship support. JC and RJ thank the EPSRC for funding (EP/T012455/1, EP/M025330/1 and EP/S002766). We thank the EPSRC for a Capital Equipment award (EP/L022613/1 and EP/R042802/1), which provided the Lord Porter Laser Laboratory Facility used in this study. J. Z. and M. M. acknowledge funding by the Deutsche Forschungsgemeinschaft *via* SFB 1249 (C06).

References

1 J. Day, S. Senthilarasu and T. K. Mallick, Improving spectral modification for applications in solar cells: A review, *Renewable Energy*, 2019, **132**, 186.
2 M. J. Y. Tayebjee, D. R. McCamey and T. W. Schmidt, Beyond Shockley–Queisser: Molecular approaches to high-efficiency photovoltaics, *J. Phys. Chem. Lett.*, 2015, **6**, 2367.
3 A. Rao and R. H. Friend, Harnessing singlet exciton fission to break the Shockley–Queisser limit, *Nat. Rev. Mater.*, 2017, **2**, 17063.
4 L. Frazer, J. K. Gallaher and T. W. Schmidt, Optimizing the efficiency of solar photon upconversion, *ACS Energy Lett.*, 2017, **2**, 1346.
5 T. Yago, K. Ishikawa, R. Katoh and M. Wakasa, Magnetic field effects on triplet pair generated by singlet fission in an organic crystal: Application of radical pair model to triplet pair, *J. Phys. Chem. C*, 2016, **120**, 27858.
6 M. I. Collins, D. R. McCamey and M. J. Y. Tayebjee, Fluctuating exchange interactions enable quintet multiexciton formation in singlet fission, *J. Chem. Phys.*, 2019, **151**, 164104.
7 D. G. Bossanyi, M. Matthiesen, S. Wang, J. A. Smith, R. C. Kilbride, J. D. Shipp, D. Chekulaev, E. Holland, J. E. Anthony, J. Zaumseil, A. J. Musser and J. Clark, Emissive spin-0 triplet-pairs are a direct product of triplet–triplet annihilation in pentacene single crystals and anthradithiophene films, *Nat. Chem.*, 2021, **13**, 163.
8 A. Neef, S. Beaulieu, S. Hammer, S. Dong, J. Maklar, T. Pincelli, R. P. Xian, M. Wolf, L. Rettig, J. Pflaum, et al., Orbital-resolved observation of singlet fission, *Nature*, 2023, **616**, 275.
9 W.-L. Chan, M. Ligges, A. Jailaubekov, L. Kaake, L. Miaja-Avila and X.-Y. Zhu, Observing the multiexciton state in singlet fission and ensuing ultrafast multielectron transfer, *Science*, 2011, **334**, 1541.
10 H. Najafov, B. Lee, Q. Zhou, L. C. Feldman and V. Podzorov, Observation of long-range exciton diffusion in highly ordered organic semiconductors, *Nat. Mater.*, 2010, **9**, 938.
11 P. Irkhin and I. Biaggio, Direct imaging of anisotropic exciton diffusion and triplet diffusion length in rubrene single crystals, *Phys. Rev. Lett.*, 2011, **107**, 017402.

12 P. Irkhin, A. Ryasnyanskiy, M. Koehler and I. Biaggio, Absorption and photoluminescence spectroscopy of rubrene single crystals, *Phys. Rev. B: Condens. Matter Mater. Phys.*, 2012, **86**, 085143.
13 W. Kim and A. J. Musser, Tracking ultrafast reactions in organic materials through vibrational coherence: vibronic coupling mechanisms in singlet fission, *Adv. Phys.: X*, 2021, **6**, 1918022.
14 S. Tao, H. Matsuzaki, H. Uemura, H. Yada, T. Uemura, J. Takeya, T. Hasegawa and H. Okamoto, Optical pump-probe spectroscopy of photocarriers in rubrene single crystals, *Phys. Rev. B: Condens. Matter Mater. Phys.*, 2011, **83**, 75204.
15 L. Ma, K. Zhang, C. Kloc, H. Sun, M. E. Michel-Beyerle and G. G. Gurzadyan, Singlet fission in rubrene single crystal: direct observation by femtosecond pump–probe spectroscopy, *Phys. Chem. Chem. Phys.*, 2012, **14**, 8307.
16 L. Ma, G. Galstyan, K. Zhang, C. Kloc, H. Sun, C. Soci, M. E. Michel-Beyerle and G. G. Gurzadyan, Two-photon-induced singlet fission in rubrene single crystal, *J. Chem. Phys.*, 2013, **138**, 184508.
17 G. B. Piland, J. J. Burdett, D. Kurunthu and C. J. Bardeen, Magnetic field effects on singlet fission and fluorescence decay dynamics in amorphous rubrene, *J. Phys. Chem. C*, 2013, **117**, 1224.
18 H. Tamura, M. Huix-Rotllant, I. Burghardt, Y. Olivier and D. Beljonne, First-principles quantum dynamics of singlet fission: Coherent versus thermally activated mechanisms governed by molecular π-stacking, *Phys. Rev. Lett.*, 2015, **115**, 107401.
19 K. A. Ward, B. R. Richman and I. Biaggio, Nanosecond pump and probe observation of bimolecular exciton effects in rubrene single crystals, *Appl. Phys. Lett.*, 2015, **106**, 223302.
20 Y. Ishibashi, Y. Inoue and T. Asahi, The excitation intensity dependence of singlet fission dynamics of a rubrene microcrystal studied by femtosecond transient microspectroscopy, *Photochem. Photobiol. Sci.*, 2016, **15**, 1304.
21 K. Miyata, Y. Kurashige, K. Watanabe, T. Sugimoto, S. Takahashi, S. Tanaka, J. Takeya, T. Yanai and Y. Matsumoto, Coherent singlet fission activated by symmetry breaking, *Nat. Chem.*, 2017, **9**, 983.
22 I. Breen, R. Tempelaar, L. A. Bizimana, B. Kloss, D. R. Reichman and D. B. Turner, Triplet separation drives singlet fission after femtosecond correlated triplet pair production in rubrene, *J. Am. Chem. Soc.*, 2017, **139**, 11745.
23 K. Bera, C. J. Douglas and R. R. Frontiera, Femtosecond Raman microscopy reveals structural dynamics leading to triplet separation in rubrene singlet fission, *J. Phys. Chem. Lett.*, 2017, **8**, 5929.
24 D. M. Finton, E. A. Wolf, V. S. Zoutenbier, K. A. Ward and I. Biaggio, Routes to singlet exciton fission in rubrene crystals and amorphous films, *AIP Adv.*, 2019, **9**, 95027.
25 D. G. Bossanyi, Y. Sasaki, S. Wang, D. Chekulaev, N. Kimizuka, N. Yanai and J. Clark, Spin statistics for triplet–triplet annihilation upconversion: Exchange coupling, intermolecular orientation, and reverse intersystem crossing, *JACS Au*, 2021, **1**, 2188.
26 D. G. Bossanyi, Y. Sasaki, S. Wang, D. Chekulaev, N. Kimizuka, N. Yanai and J. Clark, optimized rubrene-based nanoparticle blends for photon upconversion, singlet energy collection outcompetes triplet-pair separation, not singlet fission, *J. Mater. Chem. C*, 2022, **10**, 4684.

27 Y. Liu, X. Yang, L. Ye, H. Ma and H. Zhu, Molecular stacking controlling coherent and incoherent singlet fission in polymorph rubrene single crystals, *Aggregate*, 2023, e347, DOI: **10.1002/agt2.347**.
28 X. Xie, A. Santana-Bonilla, W. Fang, C. Liu, A. Troisi and H. Ma, Exciton–phonon interaction model for singlet fission in prototypical molecular crystals, *J. Chem. Theory Comput.*, 2019, **15**, 3721.
29 E. A. Wolf, D. M. Finton, V. Zoutenbier and I. Biaggio, Quantum beats of a multiexciton state in rubrene single crystals, *Appl. Phys. Lett.*, 2018, **112**, 83301.
30 O. D. Jurchescu, A. Meetsma and T. T. M. Palstra, Low-temperature structure of rubrene single crystals grown by vapor transport, *Acta Crystallogr., Sect. B: Struct. Sci.*, 2006, **62**, 330.
31 H.-G. Duan, A. Jha, X. Li, V. Tiwari, H. Ye, P. K. Nayak, X.-L. Zhu, Z. Li, T. J. Martinez, M. Thorwart and R. J. D. Miller, Intermolecular vibrations mediate ultrafast singlet fission, *Sci. Adv.*, 2020, **6**, eabb0052.
32 C. K. Yong, A. J. Musser, S. L. Bayliss, S. Lukman, H. Tamura, O. Bubnova, R. K. Hallani, A. Meneau, R. Resel, M. Maruyama, S. Hotta, L. M. Herz, D. Beljonne, J. E. Anthony, J. Clark and H. Sirringhaus, The entangled triplet pair state in acene and heteroacene materials, *Nat. Commun.*, 2017, **8**, 15953.
33 A. J. Musser and J. Clark, Triplet-pair states in organic semiconductors, *Annu. Rev. Phys. Chem.*, 2019, **70**, 323.
34 G. Orlandi and W. Siebrand, Theory of vibronic intensity borrowing. Comparison of Herzberg–Teller and Born-Oppenheimer coupling, *J. Chem. Phys.*, 1973, **58**, 4513.
35 A. C. Albrecht, On the theory of Raman intensities, *J. Chem. Phys.*, 1961, **34**, 1476.
36 W. G. Herkstroeter and P. B. Merkel, The triplet state energies of rubrene and diphenylisobenzofuran, *J. Photochem.*, 1981, **16**, 331.
37 F. Lewitzka and H.-G. Löhmannsröben, Investigation of triplet tetracene and triplet rubrene in solution, *Z. fur Phys. Chem.*, 1986, **150**, 69.
38 H. G. Löhmannsröben, Photophysical properties and laser performance of rubrene, *Appl. Phys. B*, 1988, **47**, 195.
39 S. R. Ellis, D. R. Dietze, T. Rangel, F. Brown-Altvater, J. B. Neaton and R. A. Mathies, Resonance Raman characterization of tetracene monomer and nanocrystals: Excited state lattice distortions with implications for efficient singlet fission, *J. Phys. Chem. A*, 2019, **123**, 3863.
40 Y. Qian, X. Li, A. R. Harutyunyan, G. Chen, Y. Rao and H. Chen, Herzberg–Teller effect on the vibrationally resolved absorption spectra of single-crystalline pentacene at finite temperatures, *J. Phys. Chem. A*, 2020, **124**, 9156.
41 Y. Qian, T. Zhang, J. Han, A. R. Harutyunyan, G. Chen, Y. Rao and H. Chen, Symmetry-breaking enhanced Herzberg–Teller effect with brominated polyacenes, *J. Phys. Chem. A*, 2021, **125**, 3589.
42 Y. Chen, B. Lee, D. Fu and V. Podzorov, The origin of a 650 nm photoluminescence band in rubrene, *Adv. Mater.*, 2011, **23**, 5370.
43 S. Tavazzi, A. Borghesi, A. Papagni, P. Spearman, L. Silvestri, A. Yassar, A. Camposeo, M. Polo and D. Pisignano, Optical response and emission waveguiding in rubrene crystals, *Phys. Rev. B: Condens. Matter Mater. Phys.*, 2007, **75**, 245416.
44 X. Wen, P. Yu, C.-T. Yuan, X. Ma and J. Tang, Singlet and triplet carrier dynamics in rubrene single crystal, *J. Phys. Chem. C*, 2013, **117**, 17741.

45 O. Mitrofanov, D. V. Lang, C. Kloc, J. M. Wikberg, T. Siegrist, W.-Y. So, M. A. Sergent and A. P. Ramirez, Oxygen-related band gap state in single crystal rubrene, *Phys. Rev. Lett.*, 2006, **97**, 166601.

46 R. J. Stöhr, G. J. Beirne, P. Michler, R. Scholz, J. Wrachtrup and J. Pflaum, Enhanced photoluminescence from self-organized rubrene single crystal surface structures, *Appl. Phys. Lett.*, 2010, **96**, 231902.

47 T. Zhu, Y. Wan, Z. Guo, J. Johnson and L. Huang, Two birds with one stone: Tailoring singlet fission for both triplet yield and exciton diffusion length, *Adv. Mater.*, 2016, **28**, 7539.

48 V. Jankus, E. W. Snedden, D. W. Bright, E. Arac, D. Dai and A. P. Monkman, Competition between polaron pair formation and singlet fission observed in amorphous rubrene films, *Phys. Rev. B: Condens. Matter Mater. Phys.*, 2013, **87**, 224202.